fibers

MDPI

Article

Mechanical and Structural Characterization of Pineapple Leaf Fiber

Eric Worlawoe Gaba [1], Bernard O. Asimeng [1], Elsie Effah Kaufmann [1], Solomon Kingsley Katu [1], E. Johan Foster [2] and Elvis K. Tiburu [1,*]

[1] Department of Biomedical Engineering, School of Engineering Sciences, University of Ghana, Accra P.O. Box LG 74, Ghana; ericgaba2009@gmail.com (E.W.G.); boasimeng@ug.edu.gh (B.O.A.); eek@ug.edu.gh (E.E.K.); skkatu@ug.edu.gh (S.K.K.)

[2] Department of Chemical and Biological Engineering, University of British Columbia, 2360 East Mall, Vancouver, BC V6T 1Z3, Canada; johan.foster@ubc.ca

* Correspondence: etiburu@ug.edu.gh

Abstract: Evidence-based research had shown that elevated alkali treatment of pineapple leaf fiber (PALF) compromised the mechanical properties of the fiber. In this work, PALF was subjected to differential alkali concentrations: 1, 3, 6, and 9% wt/wt to study the influence on the mechanical and crystal properties of the fiber. The crystalline and mechanical properties of untreated and alkali-treated PALF samples were investigated by X-ray diffractometry (XRD), Fourier transform infrared spectroscopy (FTIR), and tensile testing analysis. The XRD results indicated that crystal properties of the fibers were modified with 6% wt/wt alkali-treated PALF recording the highest crystallinity and crystallite size of 76% and 24 nm, respectively. The FTIR spectra suggested that all alkali-treated PALF samples underwent lignin and hemicellulose removal to varying degrees. An increase in the crystalline properties improved the mechanical properties of the PALF treated with alkali at 6% wt/wt, which has the highest tensile strength (1620 MPa). Although the elevated alkali treatment resulted in decreased mechanical properties of PALF, crystallinity generally increased. The findings revealed that the mechanical properties of PALF not only improve with increasing crystallinity and crystallite size, but are also dependent on the intermediate bond between adjacent cellulose chains.

Keywords: PINEAPPLE leaf fiber (PALF); crystallinity; crystal size; mechanical properties

Citation: Gaba, E.W.; Asimeng, B.O.; Kaufmann, E.E.; Katu, S.K.; Foster, E.J.; Tiburu, E.K. Mechanical and Structural Characterization of Pineapple Leaf Fiber. *Fibers* **2021**, *9*, 51. https://doi.org/10.3390/fib9080051

Academic Editor: Martin J. D. Clift

Received: 4 June 2021
Accepted: 30 July 2021
Published: 6 August 2021

1. Introduction

Sustainable green technology developments have been elevated in recent times, especially, in the polymer composite industry [1]. Thus, the focus currently is on the identification and characterization of plant fibers for a variety of applications, including fabrication of scaffolds for tissue regeneration, drug delivery, and prosthetic design [2–4]. Plant fibers have been shown to be good potential alternatives to synthetic fibers from petroleum-based non-renewable sources [5]. The use of plant fibers is attractive since they are available in abundance and their properties which include biodegradability and low density facilitate in achieving high specific strength composite designs [6]. Among the numerous plant fibers, pineapple (*Ananas comosus*) leaf fibers (PALF) which are considered agricultural waste, have shown promising properties for polymer reinforcement based on the literature [7,8].

PALF consists of about 80% cellulose, 6–12% hemicellulose, and 5–12% lignin [9,10]. Cellulose, the largest constituent of PALF, exists in two distinct forms: The crystalline and amorphous phases. In the crystalline phase, there are bundles of microfibrils, made of assemblies of (1–4) β-D-glucan chains that are strongly hydrogen-bonded [11]. The amorphous phase consists of randomly arranged cellulose and hemicellulose that contribute insignificantly to the structural and mechanical stiffness of the fiber. Therefore, several works have shown the removal of the amorphous phase through hydrolysis leading to

a higher degree of ordered crystalline regions with the ultimate goal of enhancing the stiffness of the fiber [6,12].

Research has shown that the chemical treatment of natural fibers can not only enhance their surface morphology but improve the mechanical properties of the fiber [12]. The treatment of natural fibers is related to their hydrophilic nature, which discourages good fiber-matrix bonding with the majority of hydrophobic matrixes [13]. It is for this reason that researchers in the bio-fiber space have been exploring various treatment techniques not only to improve the fibers matrix bonding ability for better composite reinforcement applications [14], but also for other reasons including the study of the effect of alkali on PALF reinforced composite's mechanical, degradation, and water uptake properties [15] and the production of nanocellulose from PALF [16].

The fiber stiffness evolvement depends on the methods and chemical concentrations in treating the fiber [12]. There are few literature reports of the use of 6% NaOH for fiber treatment and the limited mechanical properties experienced by PALF when subjected to the elevated percent NaOH treatment. However, the crystallographical information upon the percent NaOH treatment has not been well characterized. Herein, the authors seek to provide insightful information on the mechanical and crystallographical properties of PALF when subjected to differential alkaline treatments. Furthermore, information on how elevated alkali treatment of PALF limits the mechanical properties of the fiber despite the enhancement in crystallinity and crystallite size is provided in this work.

2. Materials and Method

2.1. Materials

Sodium hydroxide (NaOH) was purchased from Sigma-Aldrich (St. Louis, MO, USA). Pineapple leaves removed from the pineapple plant (*Ananas comosus*) were supplied by Mawuli Farms, Nsawam, Ghana (5.8195° North, 0.3513° West).

2.2. Methods

2.2.1. Extraction and Alkali Treatment of PALF

Matured harvested leaves of the pineapple plant were soaked in water for 4 weeks to soften the leaves for easy fiber isolation [6]. This process encouraged microorganisms including fungi and bacteria to digest the cement matrix of hemicellulose, freed the fiber bundle, and enhanced the fiber isolation (Figure 1a). The isolated fibers were washed with deionized water and air-dried (Figure 1b) for 15 days at 26 °C [17]. PALF samples were treated with different concentrations by dissolving 0.15, 0.45, 0.90, and 1.35 g of NaOH pellets in 15 g of deionized water to make: 1, 3, 6, and 9% wt/wt alkali solutions. PALF samples were immersed in the alkali solutions for 1 h at 26 °C. The fibers were picked out of the solution and rinsed with deionized water repeatedly until pH 7 was obtained followed by air-drying at 26 °C for 24 h (Figure 1c). Three parallel experiments were conducted at the four treatment conditions for characterization.

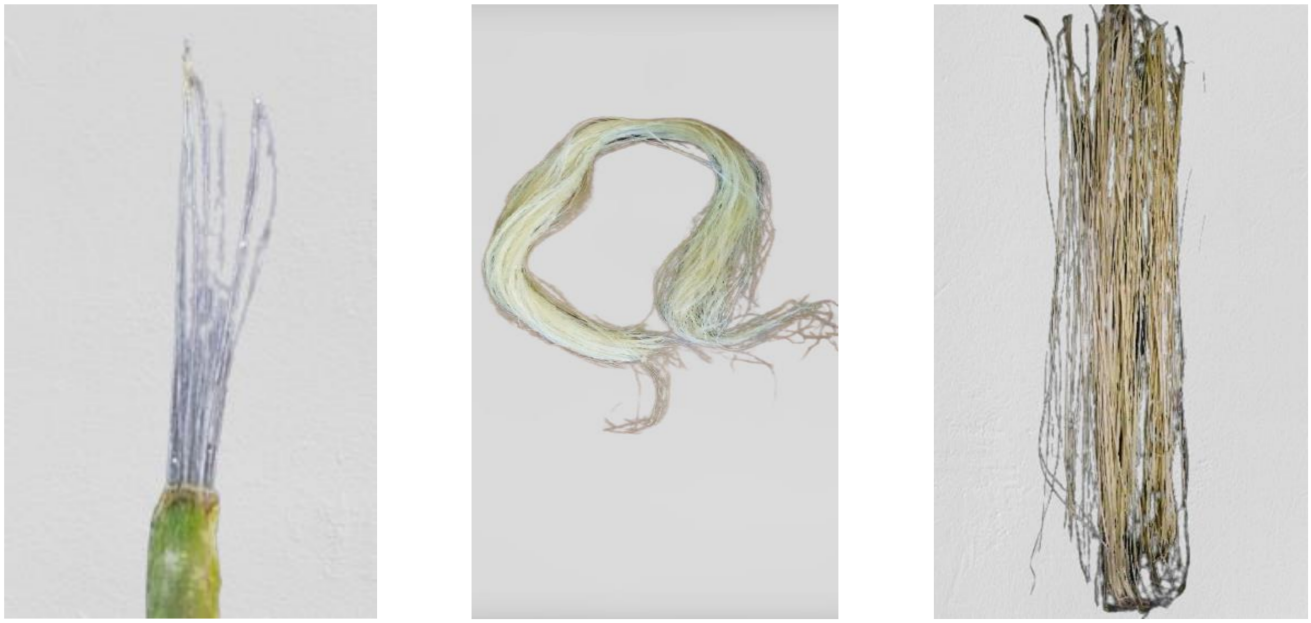

(**a**) (**b**) (**c**)

Figure 1. PALF isolation process: (**a**) Isolated fiber from the leaf; (**b**) drying at room temperature; (**c**) NaOH treated PALF.

2.2.2. Fiber Tensile Test

Tensile tests were carried out on untreated, 1, 3, 6, and 9% wt/wt NaOH treated PALF samples according to ASTM C1557-14 [18] using Mark-10 ESM301 Force Test Stand in Basic mode equipped with 1.5 kN load capacity. To avoid fiber slippage out of the holding jaws (grip), the ends of the fiber specimens were mounted and aligned on cardboards using cyanoacrylate (mounting tab). The tensile test was performed at a constant crosshead displacement rate of 20 mm/min at a relative humidity of 76% and a temperature of 26 °C. Tensile tests were conducted on fibers using a gage length of 25 mm with at least three replicates for each sample. The Force-displacement data were acquired directly using the MESUR Lite software by Mark-10 for tensile properties determination. Generally, a variation in fiber diameter for all the different NaOH treated PALF samples was observed. The fiber diameter of the fractured end within the gage length was measured using a micrometer screw gauge. The original cross-sectional area of the fractured fiber was calculated using Equation (1):

$$A = \pi \frac{d^2}{4} \tag{1}$$

where d is the diameter of the fiber and A is the cross-sectional area of the fiber. The calculated original fiber cross-section of the fractured fiber surface was used to calculate the tensile strength for each fiber tested. The average force at which each sample fractured with the original cross-sectional area (determined using Equation (1)) of each fractured sample was used to calculate the tensile strength using Equation (2):

$$Tensile\ Strength\ (\sigma) = \frac{F}{A} \tag{2}$$

where F is the tensile force experienced by the fiber at fracture and A is the original cross-sectional area of the fiber at fracture.

2.3. Characterization of PALF

2.3.1. X-ray Diffraction (XRD) Analysis

The X-ray diffraction spectrum of each powdered sample was obtained using a Pan Analytical diffractometer with monochromatic CuKα radiation (λ = 1.54060), operated at

45 kV and 40 mA. The intensities of the scattered radiation were detected in the 2θ range of 5–45°, with a scan step width of 0.05°.

The percentage crystallinity of untreated and differentially treated PALF samples was determined using the peak height empirical method (Equation (3)) proposed by [19]:

$$C = \frac{I_{002} - I_{AM}}{I_{002}} \times 100\% \quad (3)$$

where I_{002} represents the intensity of the peak corresponding to the maximum intensity of the peak; I_{AM} gives the intensity of diffraction of the non-crystalline material (amorphous band), which is taken as the valley between the crystalline peaks. Furthermore, the crystallite sizes of the samples were estimated using the Debye-Scherrer relation in Equation (4):

$$D = \frac{K\lambda}{\beta cos\theta} \quad (4)$$

where D represents the crystallite size, λ represents the wavelength of the Cu-K radiation, β represents FWHM fraction angles, K is the correction factor of 0.89, and θ represents the diffraction angle of the highest peak of the PALF samples.

2.3.2. FTIR Analysis

Untreated and differently treated PALF samples were cut into small particle sizes of about 1 mm and analyzed using Nicolet MAGNA-IR 750 Spectrometer (Nicolet Instrument Co., Madison, WI, USA). FTIR spectra were recorded with ATR attachment to determine the functional groups of the PALF before and after differential treatments. The spectra were recorded from 4000 to 500 cm^{-1} wavenumber with 16 scans and spectral resolution of 4 cm^{-1}.

2.4. Statistical Data Analysis

The data acquired was organized and analyzed using IBM SPSS Statistical Software, version 22 and the Origin 9 Data Analysis and Graphing Software. The distribution of the data was evaluated for normality assumption using Q-Q plots, Kolmogorov-Smirnov (KS), and Shapiro-Wilk tests at $p > 0.05$ before the parametric analysis was conducted. The mean and standard deviations were used to describe the data spread. One-way independent analysis of variance (ANOVA) with Tukey's HSD post hoc analysis was conducted to measure the effect of the NaOH concentration on the tensile properties of the fibers at a 0.05 significance level.

3. Results

3.1. Fiber Tensile Test

Figure 2 shows distinctive stress-strain curves obtained from a single fiber tensile testing performed on untreated and differentially treated PALF samples. Table 1 shows the ultimate tensile strength (UTS), Young's modulus, and strain at break of all PALF samples. It is observed that the strains at break of the treated PALFs are lower (<7.9%) than the untreated PALF. In addition, the treated PALFs returned higher UTS (>630 MPa) values as compared to the untreated PALF with treated PALF (6% wt/wt NaOH) recording the highest UTS of 1620 MPa. The changes in the fiber stress and strain values are indications of the increment in stiffness and the decrement in strain at break, respectively. Treated PALFs recorded higher Young's modulus as compared to the untreated PALF with treated PALFs (1, 3, and 6% wt/wt NaOH) recording $\geq$ 24 GPa. One-way ANOVA followed by Tukey's HSD test showed that the NaOH treatment had a statistically significant ($p < 0.05$) effect on the UTS, Young's modulus, and strain at break of the fiber.

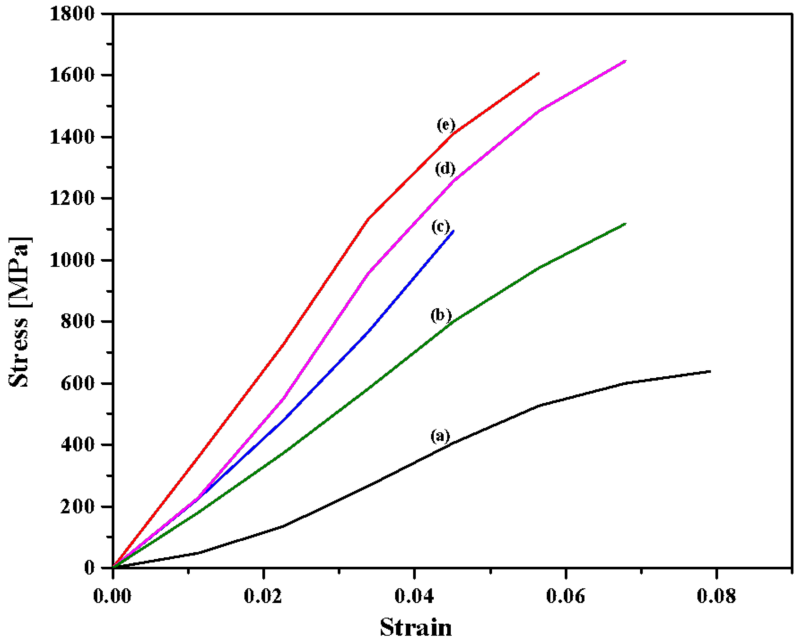

Figure 2. Stress-strain curves for (**a**) untreated PALF, (**b**) 1, (**c**) 3, (**d**) 6, and (**e**) 9% wt/wt NaOH treated PALF. The NaOH treatment of the PALF resulted in an increment in fiber UTS values and a decrement in strain at break values.

Table 1. Summary of tensile properties of untreated and NaOH treated PALF samples.

PALF Samples	Ultimate Tensile Strength (MPa)	Young's Modulus (GPa)	Strain at Break (%)
	Mean ± SD	Mean ± SD	Mean ± SD
Untreated PALF	630 ± 50 *	9 ± 1.1 *	7.9 ± 0.7 ***
1% NaOH	1560 ± 270 ***	29 ± 2.2 ****	5.6 ± 0.1 **
3% NaOH	1090 ± 166 **	24 ± 0.7 ***	4.5 ± 0.1 *
6% NaOH	1620 ± 150 ***	27 ± 0.9 ****	6.7 ± 0.5 ***
9% NaOH	1100 ± 56 **	17 ± 0.2 **	6.7 ± 0.4 ***

The *, **, ***, **** indicates a significant difference between samples at the 0.05 confidence level.

3.2. XRD Analysis: Crystallinity and Crystallite Size

Figure 3 shows XRD patterns of untreated and treated PALFs. The result indicates a similar pattern of cellulose I crystal where the most intense peak was at 22° 2θ position and corresponds to the (002) plane reflection. In addition, a minor peak at 15.1° 2θ position which corresponds to (101) plane reflection is also identified for the untreated and treated PALFs [20]. However, a peak split is observed at (101) plane reflection occurring at 15.0 and 16.6° 2θ positions for treated PALF of NaOH 9% wt/wt [20]. Table 2 presents the averaged crystallinity and crystallite size of the untreated and treated PALFs. The crystallinity of the treated PALFs (1–6% wt/wt NaOH) increased but decreased for treated PALF (9% wt/wt NaOH). The crystallite size shows a wavy (zigzag) pattern for the treated PALF (1–9% wt/wt NaOH). It increased from untreated PALF to treated PALF (1% wt/wt), decreased to PALF (3% wt/wt), increased for PALF (6% wt/wt), and decreased again for PALF (9% wt/wt).

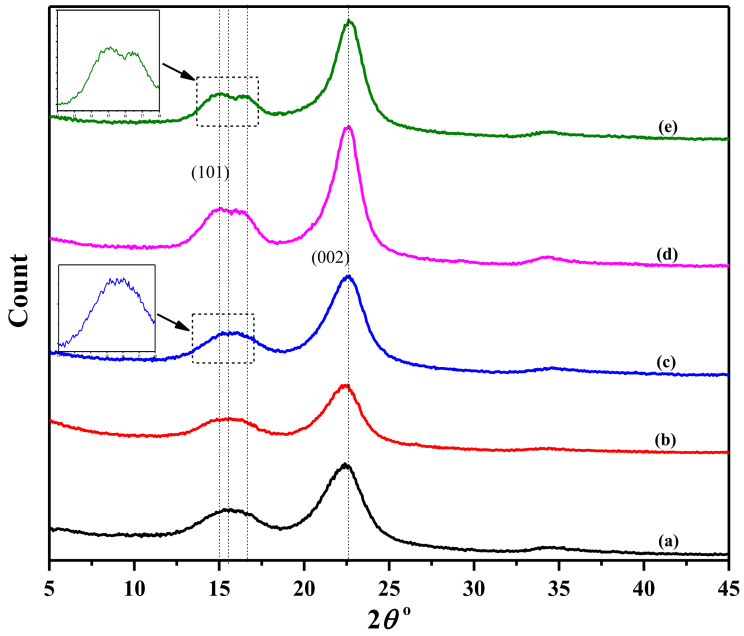

Figure 3. XRD pattern of (**a**) untreated PALF, (**b**) 1, (**c**) 3, (**d**) 6, and (**e**) 9% NaOH treated PALFs. The 9% wt/wt NaOH treatment splitted the (101) reflection peak at 15.1° 2θ position.

Table 2. Summary of crystallinity and crystallite size of untreated and differentially NaOH treated PALF samples.

PALF Sample	Crystallinity (%)	Crystallite Size (nm)
Untreated PALF	62.2	18.53
1% NaOH	65.9	21.39
3% NaOH	67.4	20.00
6% NaOH	75.6	24.00
9% NaOH	71.6	23.13

3.3. FTIR Spectral Analysis

Figure 4 shows FTIR spectra of the untreated and treated PALFs within the range of 4000–500 cm^{-1}. The spectra revealed strong absorption bands at ~3340, ~2917, ~1635, ~1426, ~1162, ~1109, and ~1030 cm^{-1}. The region at ~3340 cm^{-1} indicates bands of O-H functional groups in cellulose, the main constituent of PALF. Transmission bands at ~2917 and ~1635 cm^{-1} are identified to the C–H stretching and absorbed water, respectively [13]. The band at ~1426 cm^{-1} corresponds to O–H bending and other bands indicated at ~1162, ~1109, and ~1030 cm^{-1} correspond to the C–O–C stretch of the β-1,4-glycosidic linkage [21].

However, two observations were noted between the untreated and treated PALFs. First, a single strong band at ~1244 cm^{-1} which corresponds to C–O stretching of lignin is observed in the untreated PALF, Figure 4a. The band disappears in the subsequent spectra in Figure 4b–e and is replaced by two bands at ~1234 and ~1202 cm^{-1} which corresponds to C–OH bending [22]. The other observation was that the intensity of the strong and sharp band at ~1730 cm^{-1} which corresponds to the ester and carbonyl functional (C=O) groups in lignin and hemicellulose diminished as the NaOH concentration increased. However, the band at ~1730 cm^{-1} was retained for the 9% alkali-treated PALF. Both observations are attributed to the reaction between the lignocellulosic fiber and the NaOH [17].

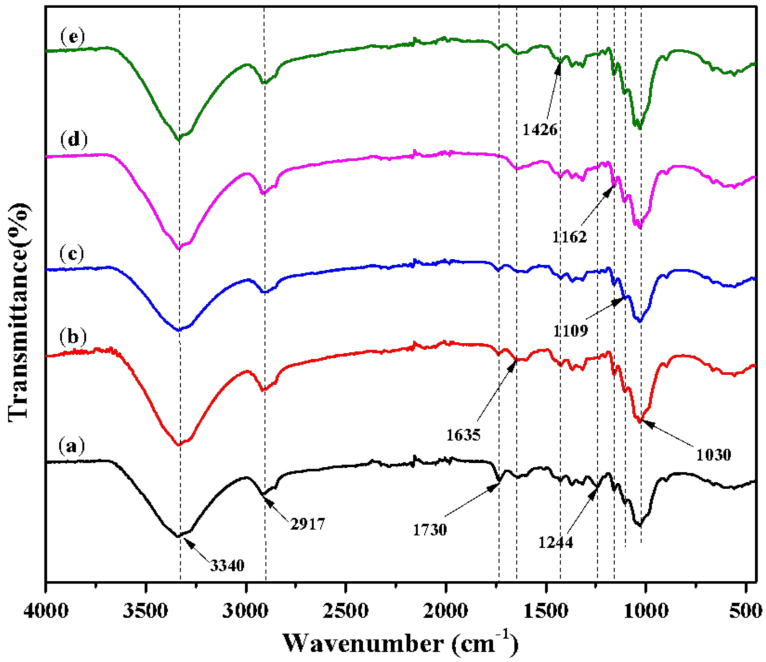

Figure 4. FTIR plot of (**a**) untreated PALF, (**b**) 1, (**c**) 3, (**d**) 6, and (**e**) 9% (wt/wt) NaOH treated PALFs. The bands at ~1244 and ~1730 cm^{-1} are affected by NaOH.

4. Discussion

4.1. The Influence of Crystal Properties on the Mechanical Behaviour of PALF

The key functional attribute of alkali treatment is to remove lignin and hemicellulose from the PALF [23]. However, the mechanical properties of natural fibers are determined by the cellulose content which is made of an ordered crystalline phase and disordered amorphous phase [24]. When the fiber is loaded, the ordered crystalline phase made of microfibrils transmits the load along the length of the fiber. Thus, the high-level ordered crystalline phase lends the advantage of superior mechanical properties to the fiber [25]. The highest UTS which was recorded for the alkali-treated PALF and agrees with the literature report [26] corroborates the XRD results. There was a common trend between changes in the crystallite size and UTS of treated PALFs. However, no common trend was identified between the UTS enhancement among the treated fibers and changes in crystallinity. It was realized that an increase in crystallinity and crystallite size of treated PALF improved the mechanical properties of the untreated PALF significantly ($p < 0.05$). The result is in good agreement with the principle that higher fiber crystallinity enhances fiber stiffness [27]. It is noticed in literature that the UTS of untreated PALF can range from 170–1627 MPa [9] and with 6–7% alkali treatment, the UTS was improved by 18–53% [12,28]. In our work, the UTS of the untreated PALF improved by 157% from 630 to 1620 MPa for the 6% alkali treatment. The variation in mechanical properties of PALF could be due to the inherent fiber properties influenced by climatic and growing conditions [6,9,27]. Whereas, crystallinity enhanced the strength and stiffness of the fiber, it decreased the strain at break which in effect was a measure of the fiber ductility [29]. Although there were reports that suggested the strength of the fiber correlates with increasing crystallinity to a limit [12,30], there is no evidential explanation of how elevated alkali treatment affects crystal properties leading to the drastic decrease in fiber strength. Therefore, in this study, it was deduced that excessive breakdown of alkali sensitive hydroxyl groups that bond adjacent cellulose chains were hydrolyzed during the alkali treatment resulting in very weak intermediate bond formation between cellulose chains. This resulted in the decreased fiber strength for the treated PALF (9% wt/wt NaOH). The decrease in fiber strength at elevated alkali treatment was also reported by other researchers where modification in the cellulose chain arrangement and the emergence of new defects at elevated alkali concentrations were

linked to the decrease in fiber strength [31,32]. Future works, therefore, would be aimed at strengthening the intermediate bonds between cellulose chains. It is interesting to note that no common trend was identified between the UTS and alkali treatment probably due to inherent structural variations among the treated fibers.

4.2. Effect of NaOH Treatment on the Crystalline Properties of PALF

The peak splitting emanated from the penetration of the crystalline regions by the high alkali treatment which scissions the long cellulose chains into shorter chains [33]. Peak splitting was intense for the 9% treatment and resulted in decreasing the crystallinity from 6%. The peak split observed in the treated PALF in our work is reported in literature for the untreated PALF [28]. The peak split that occurs with the untreated PALF could be attributed to the source of the PALF. The properties of PALF have been reported to be influenced by plant variety, growing, treatment, and climatic conditions [6,9,26]. The crystallinity of the PALF was improved as the concentration of NaOH treatment increased. It was noted that the release of acetyl groups and uronic acid substituents through hemicellulose and lignin removal further enhanced the degradation of cellulose and resulted in a lower crystallinity at the harsh treatment condition of PALF (9% wt/wt NaOH) [34]. The elevated concentration of alkali dissociated to give an excessive number of Na+ ions which aided in breaking down the crystalline regions [35,36]. Studies on the crystallite sizes from the XRD data suggested that increasing NaOH concentration generally increased the crystallite size relative to that of the untreated PALF. Line broadening at full-width-half-maximum is inversely related to the crystallite size according to Debye-Scherrer relation [37]. The decrease in crystallite size for treated PALF (3 and 9% wt/wt NaOH) could be attributed to the relatively high degree of line broadening induced by the alkali. Compared with other PALF samples, the peak at 22° was the sharpest and highest for the treated PALF (6% wt/wt NaOH) probably due to its ability to achieve the highest removal of hemicellulose and lignin constituents as indicated by the FTIR pattern [20]. The XRD result indicated a common trend between crystallinity and NaOH treatment. It was observed that the increasing concentration of NaOH achieved an increasing effect in crystallinity of PALF with the highest results realized for PALF (6% wt/wt NaOH). However, no trend was identified between the concentration of NaOH treatment and crystallite size. Structurally, lignin as a phenolic unit serves as a protective barrier encasing cellulose and hemicellulose. It is attached to the hemicellulose unit through an ester bond which is alkali sensitive. In the presence of a high concentration of NaOH, the ester bond becomes hydrolyzed, thus, exposing the hemicellulose [38]. The decrease in crystallinity and crystallite size observed for PALF (9% wt/wt NaOH) relative to PALF (6% wt/wt NaOH) might have occurred probably since at alkali concentrations above 6% wt/wt NaOH, regions of highly ordered cellulose chains of microfibrils (major reinforcing element of the fiber) became disordered due to the breakdown of alkali sensitive hydroxyl groups linking the cellulose chains in the fiber leading to decreased crystallinity. For the observed fluctuation in crystallite size, we suspect the presence of the varying number of Na^+ ions in the solution may have strained the crystalline region of the fiber at varying degrees. The strain induced possibly changed the structure of the fiber due to the presence of NaOH [34].

4.3. Effect of NaOH Treatment on the Chemical Composition of PALF

The FTIR spectrum fingerprint of untreated PALF obtained in this work was consistent with the established specific functional groups present in PALF, as reported by other researchers [39,40]. After the treatment, the unique lignin peaks disappeared followed by the appearance of additional peaks indicating the mercerization effect of the NaOH on the lignocellulosic fiber [17]. Additionally, the peak at ~1730 cm^{-1} which is characteristic of the carbonyl (C=O) absorption of the hemicellulose and lignin component of the fiber diminished as the alkali concentration increased. This is evident since the hemicellulose and lignin constituent of the fiber are alkali sensitive [41]. Moreover, it was observed that there was a progressive decrease of the peak at 1730 cm^{-1} as a function of alkali treatment up to

6%. However, upon 9% alkali treatment of the PALF, the peak at ~1730 cm^{-1} reappeared suggesting that a higher concentration of the base could be due to the ionic effect or structural variation among the fibers. The double peaks at ~1234 and ~1202 cm^{-1} might have originated from the influence of the alkali on the cellulose chains [34].

4.4. Potential Polymer Reinforcement Using PALF

The mechanical properties of PALF characterized in this work showed promising results which makes it a potential reinforcement material for matrixes such as polyester, polypropylene, and epoxy. The challenge often faced with natural fibers is the poor fiber-matrix interaction between hydrophilic fiber and hydrophobic matrix. However, the research attempts made towards fiber surface modifications, interfacial incompatibility enhancement, and tensile properties enhancement by chemical treatments such as demonstrated in this work, have shown exciting results [7,8]. The prosthetic field among the other fields has seen a limited application of PALF as a reinforcement material for prosthetic socket design. Especially in resource-limited regions of the world where accessibility and cost of materials limit amputees who are financially constrained but need prosthetic devices, the use of plant fibers such as characterized in this work can serve as an alternative to synthetic fibers. Our future work is targeted at investigating how PALF can be used to reinforce the type of prosthetic resin used for prosthetic socket design.

Additionally, the yield in PALF ranges from 1.6–2.5% per kilogram of pineapple leaf. Considering that PALF is rich in cellulose makes it a good plant material for other industries such as the paper industry. In this industry, plant sources with high cellulose content and low lignin are most preferred due to the low specific energy consumption required for the pulp refining process [42].

5. Conclusions

In this work, PALF was successfully extracted from pineapple leaves and subjected to different concentrations of alkali treatment. The removal of lignin and hemicellulose (amorphous phase) and the improvement in crystalline properties of PALF were indicated and confirmed by FTIR and XRD, respectively. These spectroscopic results were further corroborated by the high UTS recorded for the alkali-treated PALFs which ranged from 1090–1620 MPa. Although the high concentrations of NaOH improved the crystallinity and size of the PALF crystallite, it enhanced the mechanical strength and stiffness of the fiber just to a limit after which the fiber strength and stiffness drastically decreased. It was revealed that fiber strength and stiffness are not only enhanced by increased crystallinity and crystallite size, but also by the intermediate bond between adjacent crystalline chains. This work helps understand the processing conditions that could potentially allow the use of this material in a variety of matrixes, for applications ranging from aerospace, paper industry, and biomedical applications.

Author Contributions: Conceptualization, E.K.T. and B.O.A.; methodology, E.W.G., S.K.K. and B.O.A.; software, E.W.G. and S.K.K.; validation, E.K.T., B.O.A., E.E.K. and E.J.F.; formal analysis, E.W.G., S.K.K., E.K.T. and B.O.A.; investigation, E.W.G. and S.K.K.; resources, E.K.T.; original draft preparation, E.W.G., B.O.A. and E.K.T.; review and editing, B.O.A., E.E.K., E.K.T., E.J.F. and S.K.K.; supervision, E.K.T.; funding acquisition, E.J.F. All authors have read and agreed to the published version of the manuscript.

Funding: This research was funded by MENTORS FOUNDATION, grant number 200908. The APC was funded by E. Johan Foster, University of British Columbia, Vancouver, Canada.

Institutional Review Board Statement: Not applicable.

Informed Consent Statement: Not applicable.

Data Availability Statement: All data are in the paper.

Acknowledgments: We gratefully acknowledge support from MENTORS FOUNDATION, grant number 200908 from Reno, Nevada, USA.

Conflicts of Interest: The authors declare no conflict of interest.

References

1. Cislaghi, A.; Sala, P.; Borgonovo, G.; Gandolfi, C.; Bischetti, G. Towards More Sustainable Materials for Geo-Environmental Engineering: The Case of Geogrids. *Sustainability* **2021**, *13*, 2585. [CrossRef]
2. Diabor, E.; Funkenbusch, P.; Kaufmann, E.E. Characterization of Cassava Fiber of Different Genotypes as a Potential Reinforcement Biomaterial for Possible Tissue Engineering Composite Scaffold Application. *Fibers Polym.* **2019**, *20*, 217–228. [CrossRef]
3. Essel, T.Y.A.; Koomson, A.; Seniagya, M.-P.O.; Cobbold, G.P.; Kwofie, S.K.; Asimeng, B.O.; Arthur, P.K.; Awandare, G.; Tiburu, E.K. Chitosan Composites Synthesized Using Acetic Acid and Tetraethylorthosilicate Respond Differently to Methylene Blue Adsorption. *Polymers* **2018**, *10*, 466. [CrossRef] [PubMed]
4. Odusote, J.K.; Oyewo, A.T. Mechanical Properties of Pineapple Leaf Fiber Reinforced Polymer Composites for Application as a Prosthetic Socket. *J. Eng. Technol.* **2016**, *7*, 125–139.
5. Ramamoorthy, S.K.; Skrifvars, M.; Persson, A. A Review of Natural Fibers Used in Biocomposites: Plant, Animal and Regenerated Cellulose Fibers. *Polym. Rev.* **2015**, *55*, 107–162. [CrossRef]
6. Jawaid, M.; Asim, M.; Tahir, P.M.; Nasir, M. (Eds.) *Pineapple Leaf Fibers: Processing, Properties and Applications*; Green Energy and Technology; Springer: Singapore, 2020; ISBN 9789811514159.
7. Todkar, S.S.; Patil, S.A. Review on mechanical properties evaluation of pineapple leaf fibre (PALF) reinforced polymer composites. *Compos. Part B Eng.* **2019**, *174*, 106927. [CrossRef]
8. Glória, G.O.; Teles, M.C.A.; Lopes, F.P.D.; Vieira, C.M.F.; Margem, F.M.; Gomes, M.D.A.; Monteiro, S.N. Tensile strength of polyester composites reinforced with PALF. *J. Mater. Res. Technol.* **2017**, *6*, 401–405. [CrossRef]
9. Asim, M.; Abdan, K.; Jawaid, M.; Nasir, M.; Dashtizadeh, Z.; Ishak, M.R.; Hoque, M.E. A Review on Pineapple Leaves Fibre and Its Composites. *Int. J. Polym. Sci.* **2015**, *2015*, 1–16. [CrossRef]
10. Jose, S.; Salim, R.; Ammayappan, L. An Overview on Production, Properties, and Value Addition of Pineapple Leaf Fibers (PALF). *J. Nat. Fibers* **2016**, *13*, 362–373. [CrossRef]
11. Zhao, X.; Zhang, L.; Liu, D. Biomass recalcitrance. Part I: The chemical compositions and physical structures affecting the enzymatic hydrolysis of lignocellulose. *Biofuels Bioprod. Biorefin.* **2012**, *6*, 465–482. [CrossRef]
12. Asim, M.; Jawaid, M.; Abdan, K.; Nasir, M. Effect of Alkali treatments on physical and Mechanical strength of Pineapple leaf fibres. *IOP Conf. Ser. Mater. Sci. Eng.* **2018**, *290*, 12030. [CrossRef]
13. Sanjay, M.R.; Siengchin, S.; Parameswaranpillai, J.; Jawaid, M.; Pruncu, C.I.; Khan, A. A comprehensive review of techniques for natural fibers as reinforcement in composites: Preparation, processing and characterization. *Carbohydr. Polym.* **2019**, *207*, 108–121. [CrossRef]
14. Hasan, K.M.F.; Horváth, P.G.; Alpar, T. Potential Natural Fiber Polymeric Nanobiocomposites: A Review. *Polymers* **2020**, *12*, 1072. [CrossRef]
15. Hoque, M.B.; Solaiman; Alam, A.H.; Mahmud, H.; Nobi, A. Mechanical, Degradation and Water Uptake Properties of Fabric Reinforced Polypropylene Based Composites: Effect of Alkali on Composites. *Fibers* **2018**, *6*, 94. [CrossRef]
16. Mahardika, M.; Abral, H.; Kasim, A.; Arief, S.; Asrofi, M. Production of Nanocellulose from Pineapple Leaf Fibers via High-Shear Homogenization and Ultrasonication. *Fibers* **2018**, *6*, 28. [CrossRef]
17. Herrera-Franco, P.; Valadez-González, A. A study of the mechanical properties of short natural-fiber reinforced composites. *Compos. Part B Eng.* **2005**, *36*, 597–608. [CrossRef]
18. *C28 Committee Test Method for Tensile Strength and Youngs Modulus of Fibers*; ASTM International: West Conshohocken, PA, USA, 2014.
19. Segal, L.; Creely, J.J.; Martin, A.E., Jr.; Conrad, C.M. An Empirical Method for Estimating the Degree of Crystallinity of Native Cellulose Using the X-Ray Diffractometer. *Text. Res. J.* **1959**, *29*, 786–794. [CrossRef]
20. Tanpichai, S.; Witayakran, S. All-cellulose composite laminates prepared from pineapple leaf fibers treated with steam explosion and alkaline treatment. *J. Reinf. Plast. Compos.* **2017**, *36*, 1146–1155. [CrossRef]
21. Ketabchi, M.R.; Khalid, M.; Ratnam, C.T.; Manickam, S.; Walvekar, R.; Hoque, E. Sonosynthesis of cellulose nanoparticles (CNP) from kenaf fiber: Effects of processing parameters. *Fibers Polym.* **2016**, *17*, 1352–1358. [CrossRef]
22. Oh, S.Y.; Yoo, D.I.; Shin, Y.; Kim, H.C.; Kim, H.Y.; Chung, Y.S.; Park, W.H.; Youk, J.H. Crystalline structure analysis of cellulose treated with sodium hydroxide and carbon dioxide by means of X-ray diffraction and FTIR spectroscopy. *Carbohydr. Res.* **2005**, *340*, 2376–2391. [CrossRef] [PubMed]
23. Zhao, K.; Xue, S.; Zhang, P.; Tian, Y.; Li, P. Application of Natural Plant Fibers in Cement-Based Composites and the Influence on Mechanical Properties and Mass Transport. *Materials* **2019**, *12*, 3498. [CrossRef] [PubMed]
24. Petroudy, S.D. Physical and mechanical properties of natural fibers. In *Advanced High Strength Natural Fibre Composites in Construction*; Elsevier BV: Amsterdam, The Netherlands, 2017; pp. 59–83.
25. Komuraiah, A.; Kumar, N.S.; Prasad, B.D. Chemical Composition of Natural Fibers and its Influence on their Mechanical Properties. *Mech. Compos. Mater.* **2014**, *50*, 359–376. [CrossRef]
26. Neto, A.R.S.; Araujo, M.A.; Barboza, R.M.; Fonseca, A.S.; Tonoli, G.; Souza, F.; Mattoso, L.H.; Marconcini, J.M. Comparative study of 12 pineapple leaf fiber varieties for use as mechanical reinforcement in polymer composites. *Ind. Crops Prod.* **2015**, *64*, 68–78. [CrossRef]

27. Pickering, K.L.; Efendy, M.G.A.; Le, T.M. A review of recent developments in natural fibre composites and their mechanical performance. *Compos. Part A Appl. Sci. Manuf.* **2016**, *83*, 98–112. [CrossRef]
28. Jain, J.; Sinha, S.; Jain, S. Compendious Characterization of Chemically Treated Natural Fiber from Pineapple Leaves for Reinforcement in Polymer Composites. *J. Nat. Fibers* **2021**, *18*, 845–856. [CrossRef]
29. Wu, Y.; Huang, A.; Fan, S.; Liu, Y.; Liu, X. Crystal Structure and Mechanical Properties of Uniaxially Stretched PA612/SiO2 Films. *Polymers* **2020**, *12*, 711. [CrossRef]
30. Zin, M.H.; Abdan, K.; Mazlan, N.; Zainudin, E.S.; E Liew, K. The effects of alkali treatment on the mechanical and chemical properties of pineapple leaf fibres (PALF) and adhesion to epoxy resin. *IOP Conf. Ser. Mater. Sci. Eng.* **2018**, *368*, 012035. [CrossRef]
31. Duval, A.; Bourmaud, A.; Augier, L.; Baley, C. Influence of the sampling area of the stem on the mechanical properties of hemp fibers. *Mater. Lett.* **2011**, *65*, 797–800. [CrossRef]
32. Das, M.; Pal, A.; Chakraborty, D. Effects of mercerization of bamboo strips on mechanical properties of unidirectional bamboo–novolac composites. *J. Appl. Polym. Sci.* **2006**, *100*, 238–244. [CrossRef]
33. Suryanto, H.; Marsyahyo, E.; Irawan, Y.S.; Soenoko, R. Effect of Alkali Treatment on Crystalline Structure of Cellulose Fiber from Mendong (Fimbristylis globulosa) Straw. *Key Eng. Mater.* **2013**, *594*, 720–724. [CrossRef]
34. Oriez, V.; Peydecastaing, J.; Pontalier, P.-Y. Lignocellulosic Biomass Mild Alkaline Fractionation and Resulting Extract Purification Processes: Conditions, Yields, and Purities. *Clean Technol.* **2020**, *2*, 91–115. [CrossRef]
35. Cui, Z.; Shi, J.; Wan, C.; Li, Y. Comparison of alkaline- and fungi-assisted wet-storage of corn stover. *Bioresour. Technol.* **2012**, *109*, 98–104. [CrossRef] [PubMed]
36. Kumar, R.; Mago, G.; Balan, V.; Wyman, C.E. Physical and chemical characterizations of corn stover and poplar solids resulting from leading pretreatment technologies. *Bioresour. Technol.* **2009**, *100*, 3948–3962. [CrossRef] [PubMed]
37. Revol, J.F.; Dietrich, A.; Goring, D.A.I. Effect of mercerization on the crystallite size and crystallinity index in cellulose from different sources. *Can. J. Chem.* **1987**, *65*, 1724–1725. [CrossRef]
38. Reddy, K.O.; Shukla, M.; Maheswari, C.U.; Rajulu, A.V. Mechanical and physical characterization of sodium hydroxide treated Borassus fruit fibers. *J. For. Res.* **2012**, *23*, 667–674. [CrossRef]
39. Asim, M.; Jawaid, M.; Abdan, K.; Ishak, M.R. Effect of Alkali and Silane Treatments on Mechanical and Fibre-matrix Bond Strength of Kenaf and Pineapple Leaf Fibres. *J. Bionic Eng.* **2016**, *13*, 426–435. [CrossRef]
40. Samal, R.K.; Ray, M.C. Effect of Chemical Modifications on FTIR Spectra. II. Physicochemical Behavior of Pineapple Leaf Fiber (PALF). *J. Appl. Polym. Sci.* **1997**, *64*, 2119–2125. [CrossRef]
41. Wang, X.; Chang, L.; Shi, X.; Wang, L. Effect of Hot-Alkali Treatment on the Structure Composition of Jute Fabrics and Mechanical Properties of Laminated Composites. *Materials* **2019**, *12*, 1386. [CrossRef] [PubMed]
42. Małachowska, E.; Dubowik, M.; Lipkiewicz, A.; Przybysz, K.; Przybysz, P. Analysis of Cellulose Pulp Characteristics and Processing Parameters for Efficient Paper Production. *Sustainability* **2020**, *12*, 7219. [CrossRef]